(a)

(b)

Figure 4 Photograph of bottom side of micro-strip line with EBG etched in the ground plane (a) and the measured S_{21} parameters of the EBG structures (b)

verified that the novel ID-UC-EBG structure is even more compact in size as expected.

To further validate the properties of the ID-UC-EBG, two experiments concerning transmission through the above ID-UC-EBG and UC-EBG have been carried out.

First, a 2 × 5 lattice of the ID-UC-EBG is mounted on a grounded dielectric slab and connected with 50 Ω microstrip lines at both ends as a filter structure, and another similar structure is constructed using the conventional UC-EBG, the photograph of the top side of these structures is shown in Figure 3(a). As the measured results using Advantest R3767CG vector network analyzer, the S_{21} parameters of the ID-UC-EBG structure, in comparison with that of the UC-EBG structure, are shown in Figure 3(b). Evident stop-bands have been observed for both cases, the stop-band of the ID-UC-EBG structure is from 2.1 to 3.7 GHz, it is much lower than that of the UC-EBG structure as expected.

Second, a 2 × 5 lattice of the ID-UC-EBG is etched on the ground plane of a 50 Ω microstrip line, the bottom view of the microstrip structure, together with a similar structure constructed by the conventional UC-EBG, are shown in Figure 4(a). The measured S_{21} parameters of the ID-UC-EBG structures express a much lower stop-band relative to that of the conventional UC-EBG structure as shown in Figure 4(b).

4. CONCLUSION

A novel uniplanar EBG scheme, which it can be considered as an ameliorated UC-EBG surface incorporated with interdigital structure (ID-UC-EBG) is presented for size reduction. This structure significantly enlarges the fringe capacitance to compress the overall size of the structure. Its design is detailed in this article and several observations have been made from the comparisons between the ID-UC-EBG and the conventional UC-EBG, the better compactness of the novel ID-UC-EBG is verified effectively and it is shown that the ID-UC-EBG will be very valuable in practical applications.

REFERENCES

1. E. Yablonovitch, Photonic band-gap structures, J Opt Soc Am B Opt Phys 10 (1993), 283–295.
2. H.Y. David Yang, R. Kim, and D.R. Jackson, Design consideration for modeless integrated circuit substrates using planar periodic patches, IEEE Trans Microwave Theory Tech 48 (2000), 2233–2239.
3. D. Sievenpiper, L. Zhang, R.F.J. Broas, N.G. Alex′opolous, and E. Yablonovicth, High-impedance electromagnetic surfaces in a forbidden frequency band, IEEE Trans Microwave Theory Tech 47 (1999), 2059–2074.
4. Y. Qian, R. Coccioli, D. Sievenpiper, V. Radisic, E. Yablonovitch, and T. Itoh, Microstrip patch antenna using novel photonic band-gap structures, Microwave J 42 (1999), 66–76.
5. F. Yang, K. Ma, Y. Qian, and T. Itoh, A uniplanar compact photonic-bandgap (UC-EBG) structure and its applications for microwave circuits, IEEE Trans Microwave Theory Tech 47 (1999), 1509–1514.
6. F. Yang, K. Ma, Y. Qian, and T. Itoh, A novel TEM waveguide using uniplanar compact photonic-bandgap (UC-EBG) structure, IEEE Trans Microwave Theory Tech 47 (1999), 2092–2097.
7. R. Coccioli, F.R. Yang, K. Ma, and T. Itoh, Aperture coupled patch antenna on UC-EBG substrate, IEEE Trans Microwave Theory Tech 47 (1999), 2123–2130.
8. D. Gary, Inter-digital capacitors and their application to lumped-element microwave integrated circuits, IEEE Trans Microwave Theory Tech 18 (1970), 1028–1033.

A NOVEL METHOD OF DETECTING HIV/AIDS USING MICROWAVES

Anil Lonappan,[1] Vinu Thomas,[1] G. Bindu,[1] Joe Jacob,[1] C. Rajasekaran,[2] and K. T. Mathew[1]
[1] Microwave Tomography and Materials Research Laboratory, Department of Electronics, Cochin University of Science and Technology, Kochi 682 022, Kerala, India; Corresponding author: anil@cusat.ac.in
[2] Department of Medicine, Medical College, Trivandrum 695 011, Kerala, India

ABSTRACT: *HIV/AIDS is one of the most destructive epidemics in ever recorded history claims an estimated 2.4–3.3 million lives every year. Even though there is no treatment for this pandemic Elisa and Western Blot tests are the only tests currently available for detecting HIV/AIDS. This article proposes a new method of detecting HIV/AIDS based on the measurement of the dielectric properties of blood at the microwave frequencies. The measurements were made at the S-band of microwave frequency using rectangular cavity perturbation technique with the samples of blood from healthy donors as well as from HIV/*

1. INTRODUCTION

The World Health Organization estimated [1] that more than 38.6 million people now living with the HIV/AIDS disease worldwide and are transmitted through direct contact of a mucous membrane or the bloodstream with a bodily fluid containing HIV, such as blood, semen, vaginal fluid, preseminal fluid, and breast milk [2, 3]. This transmission can come in the form of anal, vaginal, or oral sex, blood transfusion, contaminated hypodermic needles, exchange between mother and baby during pregnancy, childbirth, or breastfeeding, or other exposure to one of the above bodily fluids. The symptoms of AIDS are primarily the result of conditions that do not normally develop in individuals with healthy immune systems. Most of these conditions are infections caused by bacteria, viruses, fungi, and parasites that are normally controlled by the elements of the immune system that HIV damages. Opportunistic infections are common in people with AIDS [4]. HIV affects nearly every organ system. People with AIDS also have an increased risk of developing various cancers such as Kaposi's sarcoma, cervical cancer, and cancers of the immune system known as lymphomas. Additionally, people with AIDS often have systemic symptoms of infection like fevers, sweats (particularly at night), swollen glands, chills, weakness, and weight loss [5, 6]. As HIV is a retrovirus that primarily infects vital organs of the human immune system such as $CD4^+$ T cells (a subset of T cells), macrophages, and dendritic cells. It directly and indirectly destroys $CD4^+$ T cells. $CD4^+$ T cells are required for the proper functioning of the immune system. When HIV kills $CD4^+$ T cells so that there are fewer than 200 $CD4^+$ T cells per microliter (μL) of blood, cellular immunity is lost, leading to the condition known as AIDS. Acute HIV infection progresses over time to clinical latent

TABLE 1   Variation of $CD4^+$ Cell Count in Normal and HIV/AIDS Blood Samples

Normal samples	bN1	1240 cells/μL
	bN2	920 cells/μL
	bN3	1470 cells/μL
	bN4	1030 cells/μL
HIV/AIDS samples	bA1	50 cells/μL
	bA2	125 cells/μL
	bA3	90 cells/μL
	bA4	40 cells/μL

TABLE 2   Variation Glucose in Normal and HIV/AIDS Blood Samples

Normal samples	bN1	70–105 mg/dL
	bN2	90–110 mg/dL
	bN3	75–115 mg/dL
	bN4	80–110 mg/dL
HIV/AIDS samples	bA1	25–35 mg/dL
	bA2	30–60 mg/dL
	bA3	20–30 mg/dL
	bA4	35–50 mg/dL

TABLE 3   Variation Limits of Lipid Profile in Normal and HIV/AIDS Blood Samples

	Lipid Profile	
	Normal Samples (mg/dL)	HIV/AIDS Samples (mg/dL)
T Cholesterol	<225	<125
HDL Cholesterol	<50	<150
LDL Cholesterol	<160	<100
VLDL Cholesterol	<100	<120
Triglycerides	<150	<200

HIV infection and then to early symptomatic HIV infection and later to AIDS, which is identified on the basis of the amount of $CD4^+$ T cells in the blood and the presence of certain infections. ELISA and Western Blot are a set of blood tests used in the diagnosis of chronic infection with human immunodeficiency virus (HIV). The ELISA is a screening test for the diagnosis of HIV infection. If this test is positive, it must be confirmed with a second test called the Western Blot, which is more specific and will confirm if someone is truly HIV positive because it some cases it may inaccurately produce a positive ELISA test result, including lupus, Lyme disease, and syphilis. The present study proposes a novel method of detecting HIV/AIDS based on the measurement of the dielectric properties of blood at the microwave frequencies.

The use of microwave is increasing and prevalent in various applications in diagnostic and therapeutic medicine [7]. Exhaustive studies of dielectric parameters of various human tissues and body fluids at different RF frequencies have been reported [8-10] and various measurement techniques can be adopted to measure the complex permittivity of a material and the chosen technique depends on various factors such as the nature of the sample and the frequency range used [11-14]. When only very small volumes of the sample are available, the cavity perturbation technique is an attractive option as it requires only minute volumes for the measurement [15]. The rectangular cavity perturbation technique has been employed for the measurement of the dielectric parameters of blood samples collected from healthy donors as well as from HIV/AIDS patients in this work, with the frequency range 2–3 GHz. This measurement technique is simple and quick than the conventional tests. An appreciable change is observed in the dielectric properties of patient samples than with the normal healthy samples and these measurements were in good agreement with clinical analysis. These results indicate an alternative in vitro method of diagnosing HIV/AIDS using microwaves.

2. SAMPLE PREPARATION

The blood samples were extracted by syringe from donors as well as from HIV/AIDS patients. Then it is heparin-treated sealed in

TABLE 4   Variation of Lipid Profile in Normal and HIV/AIDS Blood Samples

Sample	T Cholesterol (mg/dL)	Triglycerides (mg/dL)	HDL Cholesterol (mg/dL)	LDL Cholesterol (mg/dL)
bN1	174	112	42	132
bN2	137	127	37	126
bN3	155	110	29	145
bN4	170	139	40	117
bA1	118	172	116	68
bA2	80	142	127	49
bA3	105	154	131	73
bA4	97	167	118	88

TABLE 5 Variation of Electrolyte Profile in Normal and HIV/AIDS Blood Samples

	Electrolyte Profile (mequiv/L)	
	Normal Samples	HIV/AIDS Samples
Potassium, K	3.6–5.4 mequiv/L	1.2–2.3 mequiv/L
Magnesium, Mg	1.7 mequiv	0.85–1.1 mequiv
Sodium, Na	136–143 mequiv/L	88–95 mequiv/L
Calcium	8.5–10.5 mg/dL	2.6–2.9 mg/dL
Chloride, Cl^-	98–108 mmol/L	42–58 mmol/L
Carbon dioxide, CO_2	22–31 mmol/L	12–18 mmol/L

sample holder at 5°C to prevent coagulation and to maintain their viability. Measurements were carried out on samples which were less than 1 day old.

3. PROCEDURE

The experimental set-up consists of a transmission type S-band rectangular cavity resonator, HP 8714 ET network analyser. The cavity resonator is a transmission line with one or both ends closed. The numbers of resonant frequencies are determined by the length of the resonator. The resonator in this set-up is excited in the $TE_{10\rho}$ mode. The sample holder which is made of glass in the form of a capillary tube flared to a disk shaped bulb at the bottom is placed into the cavity through the nonradiating cavity slot, at broader side of the cavity which can facilitate the easy movement of the holder. The resonant frequency f_o and the corresponding quality factor Q_o of the cavity at each resonant peak with the empty sample holder placed at the maximum electric field are noted. The same holder filled with known amount of sample under study is again introduced into the cavity resonator through the nonradiating slot. The resonant frequencies of the sample loaded cavity are selected and the position of the sample is adjusted for maximum perturbation (i.e., maximum shift of resonant frequency

with minimum amplitude for the peak). The new resonant frequency f_s and the quality factor Q_s are noted. The same procedure is repeated for other resonant frequencies.

4. THEORY

When a material is introduced into a resonant cavity, the cavity field distribution and resonant frequency are changed which depend on shape, electromagnetic properties, and its position in the fields of the cavity. Dielectric material interacts only with electric field in the cavity.

According to the theory of cavity perturbation, the complex frequency shift is related as [15]

$$-\frac{d\Omega}{\Omega} \approx \frac{(\bar{\varepsilon}_r - 1)\int\limits_{v_s} E \cdot E_0^* dV}{2\int\limits_{V_c} |E_0|^2 dV}.$$ (1)

But

$$\frac{d\Omega}{\Omega} \approx \frac{d\omega}{\omega} + \frac{j}{2}\left[\frac{1}{Q_S} - \frac{1}{Q_0}\right].$$ (2)

Equating (1) and (2) and separating real and imaginary parts results the following:

$$\varepsilon_r' - 1 = \frac{f_o - f_s}{2f_s}\left(\frac{V_c}{V_s}\right),$$ (3)

$$\varepsilon_r'' = \frac{V_c}{4V_s}\left(\frac{Q_o - Q_s}{Q_o Q_s}\right).$$ (4)

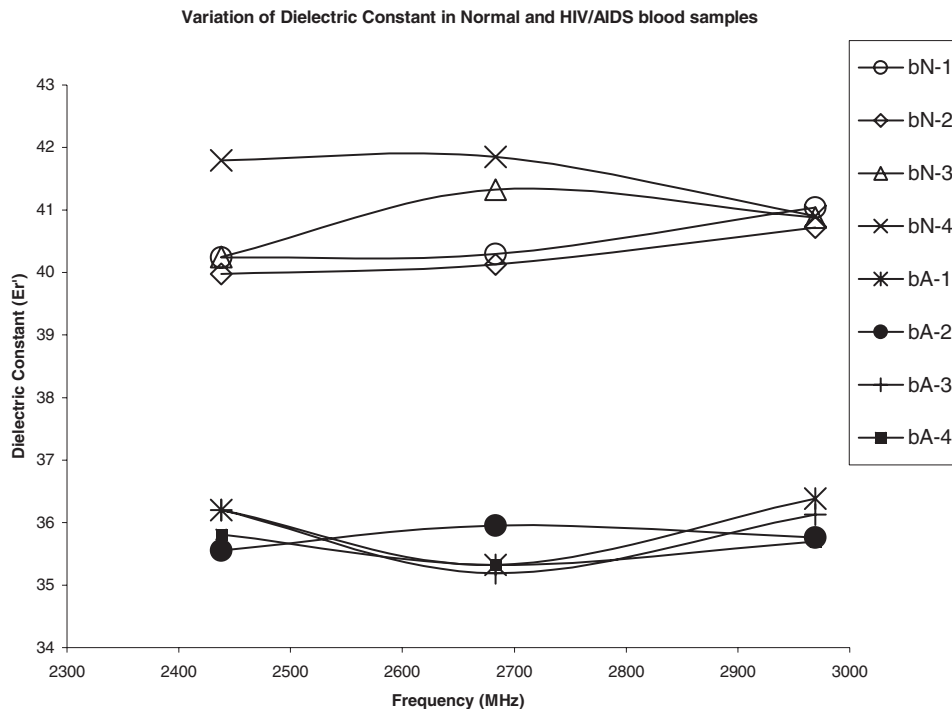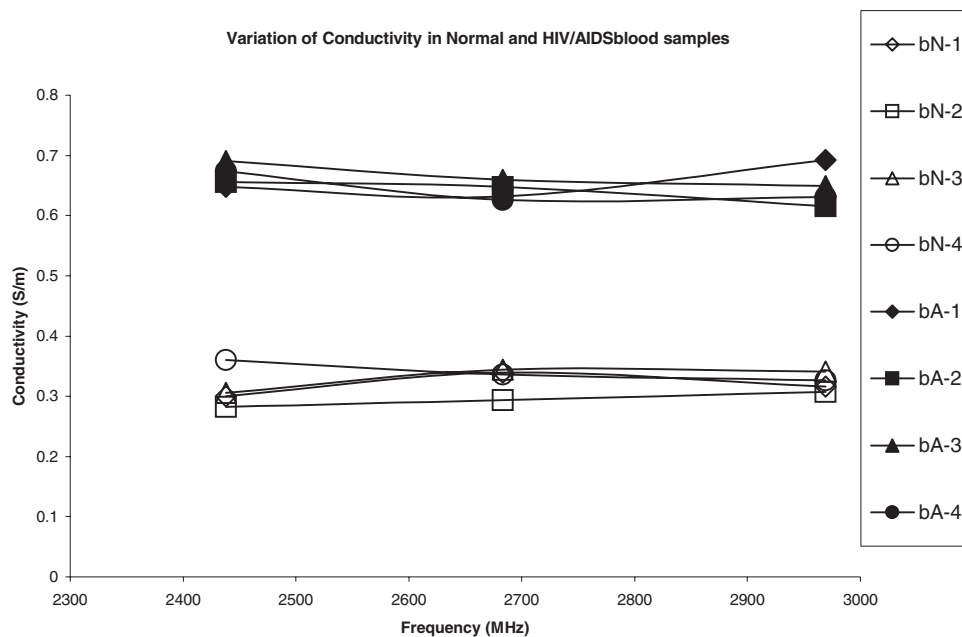**Variation of Dielectric Constant in Normal and HIV/AIDS blood samples**

Figure 1 Variation of dielectric constant in normal and HIV/AIDS blood samples

Figure 2 Variation of conductivities in normal and HIV/AIDS blood samples

Here, $\bar{\varepsilon}_r = \varepsilon'_r - j\varepsilon''_r$, $\bar{\varepsilon}_r$ is the relative complex permittivity of the sample, ε'_r is the real part of the relative complex permittivity, which is known as dielectric constant. ε''_r is the imaginary part of the relative complex permittivity associated with the dielectric loss of the material. V_s and V_c are corresponding volumes of the sample and the cavity resonator. The conductivity can be related to the imaginary part of the complex dielectric constant as

$$\sigma_e = \omega\varepsilon'' = 2\pi f\varepsilon_0\varepsilon''_r. \tag{5}$$

5. RESULTS AND DISCUSSION

Blood samples are collected from healthy donors as well as from the HIV/AIDS patients. The medical laboratories perform the clinical tests to obtain the necessary clinical parameters. The clinical laboratory parameters and the dielectric constant of blood are compared to obtain a relation. In a normal blood sample, the CD4$^+$ cell count is in the range of 500–1500 cells/μL and that of AIDS/HIV patients is in the order of 30–180 cells/μL and the clinical results are tabulated in the Table 1. These results show a remarkable and noticeable variation in CD4$^+$ cell count in normal and HIV/AIDS blood samples. Table 2 shows the results of glucose level in normal and HIV/AIDS blood samples and there is considerable variation in between the two types of blood samples. Table 3 indicates the limits of Lipid Profile in normal and HIV/AIDS blood samples, and Table 4 is the Lipid Profile results in the normal and HIV/AIDS blood samples obtained in the clinical analysis. Lipid Profile results also show a remarkable variation between the normal and HIV/AIDS blood samples. The Electrolyte Profile in normal and HIV/AIDS blood samples is tabulated in Table 5 and it shows a variation between the two types of blood samples. Figure 1 shows the Dielectric Constant variation in Normal and HIV/AIDS blood samples and the dielectric constant is more in the normal blood samples than the HIV/AIDS samples. This is attributed because of increased concentration levels of results of CD4$^+$ cells, glucose, and electrolyte levels in normal blood samples. Figure 2 shows that conductivity of HIV/AIDS blood samples is more than that of normal blood samples and this increased level of conductivity is due to the presence of HDL

Cholesterol, VLDL Cholesterol, and Triglycerides. An appreciable change is observed in the dielectric properties of HIV/AIDS samples than with the normal healthy samples and these measurements are in good agreement with clinical results. This study shows a great correlation between the laboratory results and blood diagnosis using microwaves.

6. CONCLUSION

The microwave characterization of the blood samples is done using cavity perturbation technique. The cavity perturbation technique is technique is simple, fast, and accurate and requires very low volume of samples of blood for measuring the dielectric properties. It is observed that in the specified band of frequencies, there is an appreciable change in the dielectric properties of HIV/AIDS blood samples with that of the normal healthy samples and these results are in good agreement with clinical results. This study is a novel in vitro method of diagnosing HIV/AIDS using microwaves.

REFERENCES

1. WHO, Overview of the global AIDS epidemic, Chapter 2,WHO Geneva, Switzerland, 2006, pp. 8-50.
2. HIV and its transmission, Report by Divisions of HIV/AIDS Prevention, Centers for Disease Control and Prevention, United States Department of Health and Human Services, Atlanta, Georgia, 2003.
3. How HIV is spread, Report by San Francisco AIDS Foundation, San Francisco, CA, 2006.
4. C.B. Holmes, E. Losina, R.P. Walensky, Y. Yazdanpanah, K.A. Freedberg, Review of human immunodeficiency virus type 1-related opportunistic infections in sub-Saharan Africa, Clin Infect Dis 36 (2003), 656-662.
5. D.A. Guss, The acquired immune deficiency syndrome: an overview for the emergency physician, Part 1, J Emerg Med 12 (1994), 375-384.

6. D.A. Guss, The acquired immune deficiency syndrome: an overview for the emergency physician, Part 2, J Emerg Med 12 (1994), 491-497.

7. Special issues, IEEE Trans Microwave Theory Tech 50 (2002).

8. S. Gabriel, R.W. Lau, and C. Gabriel, The dielectric properties of biological tissues. II. Measurements on the frequency range 10 Hz to 20 GHz, Phys Med Biol 41 (1996), 2251-2269.

9. H.F. Cook, Dielectric behavior of human blood at microwave frequencies, Nature 168 (1951), 247-248.

10. H.F. Cook, The dielectric behavior of some types of human tissues at microwave frequencies, Br J Appl Phys 2 (1951), 295-300.

11. D.K. Ghodgaonkar, V.V. Varadan, and V.K. Varadan, Free space measurement of complex permittivity and complex permeability of magnetic materials at microwave frequencies, IEEE Trans Instrum Meas 19 (1990), 387-394.

12. D.K. Ghodgaonkar, V.V. Varadan, and V.K. Varadan, A free space method for measurement of dielectric constant and loss tangents at microwave frequencies, IEEE Trans Instrum Meas 38 (1989), 789-793.

13. W. Barry, A broadband, automated, stripline technique for the simultaneous measurement of complex permittivity and complex permeability, IEEE Trans Microwave Theory Tech 34 (1986), 80-84.

14. Z. Abbas, R.D. Pollard, and R.W. Kelsall, A rectangular dielectric waveguide technique for determination of permittivity of materials at W-band, IEEE Trans Microwave Theory Tech 46 (1998), 2011-2015.

15. K.T. Mathew, Perturbation theory, Encyclopedia of RF and Microwave Engineering, Vol. 4, Wiley-Interscience, USA, 2005, pp. 3725-3735.

THE REALIZATION AND ANALYSIS OF PATTERN/POLARIZATION DIVERSITY IN MULTIPLE INPUT MULTIPLE OUTPUT ARRAY

Sung Ho Chae, Hyeong-Sik Yoon, and Seong-Ook Park
School of Engineering, Information and Communications University (ICU), Daejeon, Korea; Corresponding author: slapguitar@icu.ac.kr

ABSTRACT: *This article proposes the pattern/polarization diversity array for multiple input multiple output applications by applying vertical and horizontal excitation. We show that pattern and polarization of antenna are changed due to vertical feeding. Then, we attempt to realize the two antenna diversity array by using different feeding method. As a result, the correlation factors with respect to the pattern and polarization diversity are investigated. Finally, the analysis of the diversity system in the view point of capacity is presented.* © 2008 Wiley Periodicals, Inc. Microwave Opt Technol Lett 50: 561–566, 2008; Published online in Wiley InterScience (www.interscience.wiley.com). DOI 10.1002/mop. 23142

1. INTRODUCTION

Recently, multiple input multiple output (MIMO) systems have received a great attention for their ability to overcome the limits of SISO channel capacity [1]. They provide a very high spectral efficient by using multiple transmitter and receiver. However, the spatial correlation between antennas causes the loss of spectral efficiency. To reduce the spatial correlation, the space, polarization, and pattern diversity techniques are most widely used. The distance between antennas needs to be multiple of the wavelength to achieve spatial multiplexing [2], so the size of ground must be much larger than typical compact MIMO arrays. Thus, space diversity technique is not suitable for 4G-wireless handsets. Instead, pattern/polarization diversity might be practical solutions to reduce the array size.

The technique of changing the antenna pattern/polarization by using two different feed ports, vertical and horizontal feeding, is recently reported [3]. As the feeding directions are changed, the components of copolarization are changed. For instance, if we assume that antennas are located in y–z plane, E_ϕ is the copolarization component in horizontal feeding while the cross-polarization radiation in vertical feeding. This technique has the advantage that dose not need the additional circuit for changing the main radiation direction. By applying these techniques, the authors proposed pattern/polarization diversity system for dual band operation which can apply to worldwide interoperability for microwave access (WiMAX) application in 2.6 GHz and wireless local area network (WLAN) systems in 5.2 GHz. In addition, we presented the analysis of the diversity system in the view point of capacity and the benefit of the proposed diversity system compared to horizontal excitation.

2. THEORETICAL BACKGROUND

The instantaneous ergodic channel capacity of MIMO with equal-power allocation has been shown to be [1]

$$C(H) = \log_2 \det\left(I + \frac{P}{T\sigma_N^2} HH\dagger\right) \tag{1}$$

where P/σ_N^2 is the signal to noise ratio, H is channel matrix, and T denotes the number of transmit antennas. Since H is randomly changed, the capacity is also random variable. Therefore, we can quantify the capacity by complementary cumulative distribution function (CCDF). In case of the correlated Rayleigh channel, H can be factorized in form as follows [4]:

$$H = (\Psi^R)^{1/2} W (\Psi^T)^{1/2} \tag{2}$$

where Ψ^R and Ψ^T are the correlation matrix of transmit antennas and receive antennas, respectively and the entries of W are independent and identically distributed (i.i.d) complex circular symmetric Gaussian with mean 0 and variance 1. In this article, transmit antennas are assumed to be uncorrelated and only receive sides are correlated (one sided correlation channel model). Also, the incoming waves from base station are assumed to have the unity cross polar discrimination (XPD).

The entries of covariance matrix Ψ^R is defined by the following equation [5],

$$\Psi_{ij}^R = \frac{1}{\sigma_i \sigma_j} \oint \{E_{i\theta}^*(\theta,\phi) E_{j\theta}(\theta,\phi)$$
$$+ E_{i\phi}^*(\theta,\phi) E_{j\phi}(\theta,\phi)\} P(\theta,\phi) e^{j\Phi_{i,j(\Omega)}} d\Omega \tag{3}$$

where $E(\theta,\phi)$ and $P(\theta,\phi)$ are complex far-field patterns of the received antennas and the distribution of angle-of-arrival (AoA) of incoming waves, respectively. We assume the uniform AoA distributions, and they are independent in terms of θ and ϕ directions. In addition, σ_i and σ_j are the standard deviations of each received signal. They can be expressed by following equations.

$$\sigma^2 = \oint \{|E_\theta(\theta,\phi)|^2 + |E_\phi(\theta,\phi)|^2\} P(\theta,\phi) d\Omega \tag{4}$$